

Mutual-Guided Expert Collaboration for Cross-Subject EEG Classification

Zhi Zhang¹, Yan Liu^{1,*}, Zhejing Hu¹, Gong Chen², Jiannong Cao¹, Shenghua Zhong³, Sean Fontaine², Changhong Jing^{1,4} and Shuqiang Wang⁴

¹The Hong Kong Polytechnic University, Hong Kong, China

²Biaohan Limited, Shenzhen, China

³Shenzhen University, Shenzhen, China

⁴Shenzhen Institutes of Advanced Technology, Shenzhen, China

{zhi271.zhang, zhejing.hu, changhong.jing}@connect.polyu.hk, {yan.liu, jiannong.cao}@polyu.edu.hk, heinz.g.chen@hotmail.com, csshzhong@szu.edu.cn, sean@clozzz.com, sq.wang@siat.ac.cn

Abstract

Decoding the human brain from electroencephalography (EEG) signals holds promise for understanding neurological activities. However, EEG data exhibit heterogeneity across subjects and sessions, limiting the generalization of existing methods. Representation learning approaches sacrifice subject-specific information for domain invariance, while ensemble learning methods risk error accumulation for unseen subjects. From a theoretical perspective, we reveal that the applicability of these paradigms depends on the reducibility cost of domain-specific functions to domain-invariant ones. Building on this insight, we propose a Mutual-Guided Expert Collaboration (MGEC) framework that employs distinct network structures aligned with domain-specific and domain-invariant functions. Shared expert-guided learning captures reducible domain-invariant functions. Routed expert-guided learning employs a mixture-of-experts architecture to model irreducible domain-specific functions. Mutual-guided learning enables collaborative regularization to prevent over-reduction and under-reduction. We validate our theoretical findings on synthetic datasets, and experiments on seven benchmarks demonstrate that MGEC outperforms state-of-the-art methods.

1 Introduction

Decoding the human brain with machine learning methods has the potential to unlock a deeper understanding of neurological activities and diagnoses [Kessler *et al.*, 2025]. A non-invasive method to collect data is electroencephalography (EEG), which measures the brain’s electrical activity using electrodes placed on the scalp [Schalk *et al.*, 2004]. Known for its high temporal resolution, EEG captures rapid changes in brain activities, making it valuable for both research and clinical examinations. By analyzing patterns in EEG signals, classification models have been developed to identify specific brain states.

*Corresponding author

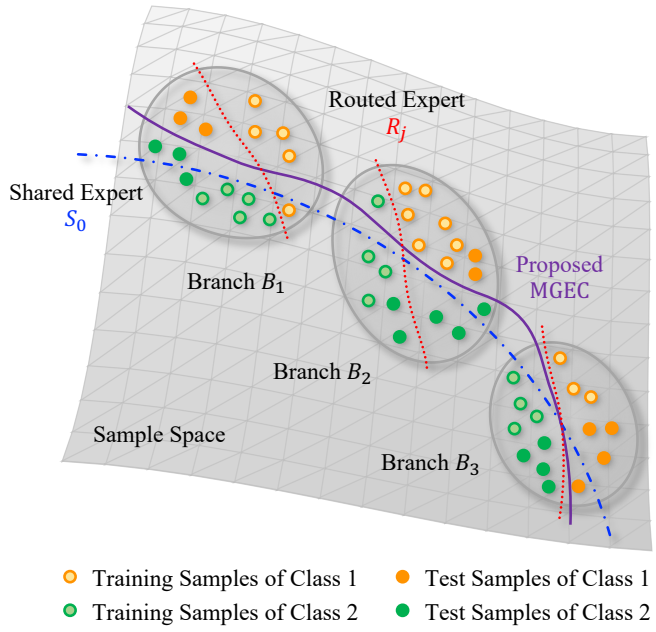


Figure 1: The illustration of shared expert and routed expert behaviors on heterogeneous EEG data.

Over the past decades, a variety of deep learning networks have been proposed for specific datasets and applications in brain-computer interaction, including convolutional neural networks, recurrent neural networks, and transformers. These models have achieved success in single-task scenarios, including emotion recognition, motor imagery classification, sleep staging, and auditory attention decoding [Sun *et al.*, 2025; Chen *et al.*, 2025; Zhou *et al.*, 2025a; Fan *et al.*, 2025].

More recently, pre-trained models have broken through limitations of different EEG task types and obtained universal perceptual capabilities of EEG signals through unsupervised pre-training in cross-task and cross-dataset scenarios [Jiang *et al.*, 2024; Wang *et al.*, 2025; Wang *et al.*, 2024a; Zhou *et al.*, 2025b].

Despite these advancements, a fundamental challenge per-

sists for both single-task and cross-task models: cross-subject generalization. EEG signals exhibit significant variations in neural patterns across subjects. Individual differences in brain anatomy and physiology lead to distinct neural patterns across individuals [Wang *et al.*, 2024e]. When such distribution shifts occur, deep learning models suffer from performance degradation, undermining the performance of models trained on one set of subjects when applied to new, unseen subjects.

To tackle cross-subject generalization, extensive efforts have been made over decades [Handiru and Prasad, 2016; Li *et al.*, 2018; Ma *et al.*, 2019; Shen *et al.*, 2022]. One line of research aims to learn subject-invariant features so that a single classifier can transfer to unseen subjects [Wang *et al.*, 2024e; Wang *et al.*, 2024c]. However, when the source domains become diverse, learning a domain-invariant model becomes increasingly challenging. Another line of research employs multiple experts: each classifier serves as an expert for its own subject, forming an ensemble; they can leverage complementary information from each other [Zhang *et al.*, 2024; Wang *et al.*, 2024d; Zhao *et al.*, 2024a]. However, the increased complexity of ensemble models poses coordination challenges, e.g., expert routing [Rane *et al.*, 2024; Mienye and Swart, 2025]. Based on these observations, a natural question arises: can we design a collaborative framework that leverages the complementary strengths of both paradigms?

We analyze this question from a theoretical perspective based on algorithmic alignment. Our analysis reveals that model generalization depends on the target function. A shared expert aligns well with branch-independent functions, while routed experts align with branch-dependent functions. Treating each domain as a branch, the choice between a shared expert and routed experts depends on the reducibility cost of branch-specific functions to branch-invariant ones. As shown in Fig. 1, when this cost is minor, e.g., strategies are homogeneous across regions, the shared expert generalizes effectively. When strategies are heterogeneous and the reducibility cost is high, routing to different experts achieves better alignment. We further show that collaborative learning constrains the risk of over-reduction and under-reduction, enabling learning in a self-paced fashion.

To this end, we propose a Mutual-Guided Expert Collaboration (MGECC) framework that implements the conclusions from our theoretical analysis. In shared expert-guided learning, the model is trained with a shared expert. We use augmented temporal neighbors as a proxy for extrapolation, encouraging the model to align with the target function under distribution shift. In routed expert-guided learning, routed experts are trained using a mixture-of-experts architecture, where each expert specializes in classifying a specific group of subjects, routing inputs to appropriate experts based on distinct processing strategies. In mutual-guided learning, the shared expert and routed experts mutually transfer knowledge by measuring the learnability of training samples and reweighting them accordingly. Samples that one model finds easier but the other finds challenging are assigned higher weights, ensuring that each expert learns from the better-performing one. During inference, the shared expert and routed experts fuse their decisions to produce the final pre-

diction.

2 Theoretical Analysis

Given source domain training data, one paradigm trains a shared expert on a unified source domain, while another routes to multiple experts across different source domains; both aim to generalize to unseen target domains. A natural question arises: what are the distinct roles of these two paradigms, and can they collaborate? This section provides theoretical analysis based on algorithmic alignment [Xu *et al.*, 2020].

Definition 1. Let \mathcal{N} denote a neural network composed of n modules $\{\mathcal{N}_i\}_{i=1}^n$, and assume that a target function g can be decomposed into n sub-functions such that $g = f_n \circ \dots \circ f_1$. We say that \mathcal{N} aligns with g if replacing each module \mathcal{N}_i with f_i yields the same output as g . The alignment measure is defined as $\text{Align}(\mathcal{N}, g, \epsilon, \delta) := n \cdot \max_{i \in [n]} \mathcal{M}(f_i, \mathcal{N}_i, \epsilon, \delta)$, where $\mathcal{M}(f_i, \mathcal{N}_i, \epsilon, \delta)$ denotes the sample complexity for \mathcal{N}_i to learn f_i with precision ϵ and failure probability δ .

Definition 1 shows that a well-aligned architecture decomposes the problem into simpler sub-problems, reducing sample complexity. We now extend algorithmic alignment [Xu *et al.*, 2020; Li *et al.*, 2023] to domain generalization under distribution shift.

Assumption 1. Let p_{tr} and p_{te} denote the training and test feature distributions at the output of \mathcal{N}_1 . There exist constants $C \geq 1$ and $\eta \geq 0$ such that for any measurable set A , $\mathbb{P}_{D_{\text{te}}}[\mathcal{N}_1(\mathbf{x}) \in A] \leq C \cdot \mathbb{P}_{D_{\text{tr}}}[\mathcal{N}_1(\mathbf{x}) \in A] + \eta$.

Remark. Subject-invariant physiological patterns ensure a bounded density ratio C , while training on diverse subjects yields a reasonable transfer error η [Berry *et al.*, 2017; Bomatter and Gouk, 2025].

Assumption 2. There exists a function g_c such that $g_c(\mathcal{N}_1(\mathbf{x})) = y$ for all $\mathbf{x} \in \mathcal{E}_{\text{tr}}$, and $\mathbb{P}_{D_{\text{te}}}[\|g_c(\mathcal{N}_1(\mathbf{x})) - y\| \leq \epsilon] \geq 1 - \delta$.

Remark. The function g_c represents correlations that persist across both training and test distributions.

Assumption 3. There exists a function g_s such that $g_s(\mathcal{N}_1(\mathbf{x})) = y$ for all $\mathbf{x} \in \mathcal{E}_{\text{tr}}$, and $\mathbb{P}_{D_{\text{te}}}[\|g_s(\mathcal{N}_1(\mathbf{x})) - y\| > \omega(\epsilon)] \geq 1 - \delta$.

Remark. The function g_s represents correlations present in training but absent in test distributions.

The following theorem extends algorithmic alignment from i.i.d. generalization to domain generalization under distribution shift.

Theorem 1. Let $\mathcal{N}' = \{\mathcal{N}_2, \dots, \mathcal{N}_n\}$. Suppose we train the neural network with ERM and Assumptions 1–3 hold. Then:

- (a) If $\text{Align}(\mathcal{N}', g_c, \epsilon, \delta) \leq |\mathcal{E}_{\text{tr}}|$, then $\mathbb{P}_{D_{\text{te}}}[\|\mathcal{N}(\mathbf{x}) - y\| \leq O(\epsilon)] \geq 1 - O(\delta) - \eta$.
- (b) If $\text{Align}(\mathcal{N}', g_s, \epsilon, \delta) \leq |\mathcal{E}_{\text{tr}}|$, then $\mathbb{P}_{D_{\text{te}}}[\|\mathcal{N}(\mathbf{x}) - y\| > \omega(\epsilon)] \geq 1 - O(\delta) - \eta$.

Remark. Networks aligned with invariant correlations generalize robustly, while those aligned with spurious correlations fail on unseen domains.

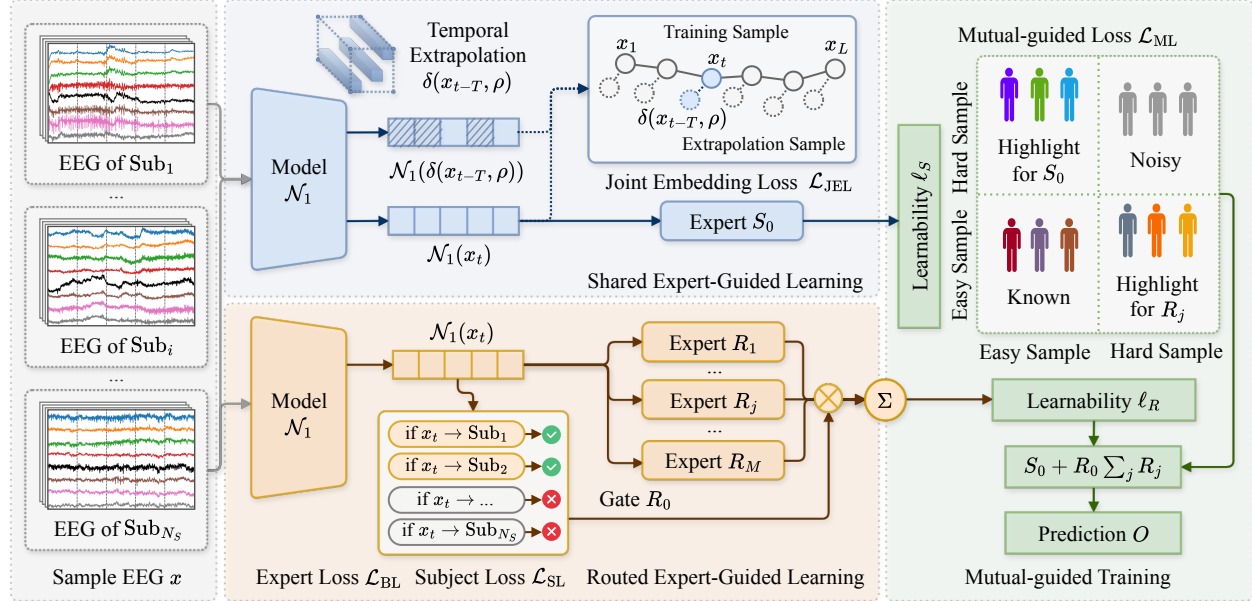


Figure 2: The framework of the proposed Mutual-Guided Expert Collaboration (MGECC) framework.

Next, we analyze the impact of the shared expert and routed experts.

Definition 2. Let g denote a target function with a branching structure $g(\mathbf{x}) = \sum_{j=1}^M \mathbf{1}_{I_j}(h_0(\mathbf{x})) \cdot h_j(\mathbf{x})$, where h_0 is a branching function that determines which branch to activate, $\{I_j\}_{j=1}^M$ are disjoint intervals partitioning the range of h_0 , and $\{h_j\}_{j=1}^M$ are branch-dependent functions. A routed expert network \mathcal{R} consists of M routed experts $\{R_j\}_{j=1}^M$ and a router R_0 , where each routed expert R_j learns h_j and the router R_0 learns h_0 . A shared expert network \mathcal{S} consists of a single shared expert S_0 that learns the entire function g .

Remark. The branching structure captures branch-dependent processing strategies, which commonly arise under distribution shift due to subject heterogeneity.

Theorem 2. Let $\mathcal{M}(R_j, h_j, \epsilon, \delta)$ and $\mathcal{M}(R_0, h_0, \epsilon, \delta)$ denote the sample complexity for routed expert R_j to learn h_j and for router R_0 to learn h_0 , respectively, with precision ϵ and failure probability δ . Let $\mathcal{M}(S_0, g, \epsilon, \delta)$ denote the sample complexity for shared expert S_0 to learn g . Let α, β with $1 \leq \alpha \leq \beta$ satisfy $\alpha \cdot \max_j \mathcal{M}(R_j, h_j, \epsilon, \delta) \leq \mathcal{M}(S_0, g, \epsilon, \delta) \leq \beta \cdot \max_j \mathcal{M}(R_j, h_j, \epsilon, \delta)$. Suppose the branching function is no harder to learn than the branch-dependent functions, i.e., $\mathcal{M}(R_0, h_0, \epsilon, \delta) \leq \max_j \mathcal{M}(R_j, h_j, \epsilon, \delta)$. Then:

- If $\alpha \geq M + 1$, then $\text{Align}(\mathcal{R}, g, \epsilon, \delta) \leq \text{Align}(\mathcal{S}, g, \epsilon, \delta)$.
- If $\beta \leq M + 1$, then $\text{Align}(\mathcal{R}, g, \epsilon, \delta) \geq \text{Align}(\mathcal{S}, g, \epsilon, \delta)$.

Remark. The ratio α (or β) reflects the reducibility cost of branch-specific functions to a branch-invariant one. When this cost is low (small β), the shared expert aligns better. When it is high (large α), routed experts achieve better alignment.

Finally, we analyze the collaboration between the shared

expert and routed experts to constrain the risk of over-reduction and under-reduction.

Assumption 4. For any sample \mathbf{x} , at least one expert produces a prediction close to the target function, i.e., $\min\{\|S(\mathbf{x}) - g(\mathbf{x})\|, \|R(\mathbf{x}) - g(\mathbf{x})\|\} \leq \varepsilon$, where ε is a small constant.

Remark. This follows from Theorem 2: at least one expert aligns well for each sample.

Theorem 3. Define the alignment errors of the shared expert and routed experts at epoch t as $\epsilon_S^{(t)} = \|S^{(t)}(\mathbf{x}) - g(\mathbf{x})\|^2$ and $\epsilon_R^{(t)} = \|R^{(t)}(\mathbf{x}) - g(\mathbf{x})\|^2$, respectively, where $g(\mathbf{x})$ denotes the target function. Under Assumption 4, the total alignment error satisfies $\mathbb{E}[\epsilon_S^{(t)} + \epsilon_R^{(t)}] \leq \mathbb{E}[\epsilon_S^{(0)} + \epsilon_R^{(0)}]$.

Remark. The expert with higher loss learns from the better-performing one, avoiding over-reduction and under-reduction.

3 Methodology

As shown in Fig. 2, we propose a Mutual-Guided Expert Collaboration (MGECC) framework. Based on the theoretical analysis in Section 2, the framework integrates a shared expert and routed experts that collaborate to process heterogeneous EEG samples. In the following subsections, we detail the three guided learning stages.

3.1 Shared Expert-Guided Learning

As established in Theorem 2, when branch-dependent functions are homogeneous across input regions, a shared expert achieves better alignment with the target function. This motivates training a single domain-agnostic classifier that pools labeled data from all source domains.

Given a batch of EEG signals, we train a shared expert S_0 by minimizing the empirical risk across all subjects using cross-entropy loss:

$$\mathcal{L}_{\text{ERM}} = -\frac{1}{N_B} \sum_{i=1}^{N_B} \sum_{c=1}^C y_{ic} \log(\hat{y}_{ic}) \quad (1)$$

where N_B is the batch size, C is the number of classes, and $y_{ic} \in \{0, 1\}$ is the ground-truth indicator for sample i belonging to class c .

To bound the transfer error η under distribution shift, we construct augmented temporal neighbors as a proxy for unseen samples whose distributional distance from training data remains controlled. For each EEG sample $\mathbf{x}^{(t)} \in \mathbb{R}^{E \times L}$, where E is the number of electrodes and L is the segment length, we retrieve its preceding consecutive T -second segment $\mathbf{x}^{(t-T)}$ of the same class. We then apply a stochastic spatial masking operation $\delta(\cdot, \rho)$ that randomly masks electrodes with probability ρ , yielding $\tilde{\mathbf{x}}^{(t-T)} = \delta(\mathbf{x}^{(t-T)}, \rho)$.

Let $\mathcal{N}_1(\cdot)$ denote the feature extractor. We obtain the representations $\mathbf{z}^{(t-T)} = \mathcal{N}_1(\tilde{\mathbf{x}}^{(t-T)})$ and $\mathbf{z}^{(t)} = \mathcal{N}_1(\mathbf{x}^{(t)})$. The joint embedding loss is defined as:

$$\mathcal{L}_{\text{JEL}} = \frac{1}{N_B} \sum_{i=1}^{N_B} \left(1 - \frac{\mathbf{z}_i^{(t-T)} \cdot \mathbf{z}_i^{(t)}}{\|\mathbf{z}_i^{(t-T)}\| \|\mathbf{z}_i^{(t)}\|} \right) \quad (2)$$

which minimizes the cosine distance between the representations of the current segment and its spatially-masked temporal neighbor.

The total loss for shared expert-guided learning is:

$$\mathcal{L}_S = \mathcal{L}_{\text{ERM}} + \mathcal{L}_{\text{JEL}} \quad (3)$$

3.2 Routed Expert-Guided Learning

As established in Theorem 2, when branch-dependent functions are heterogeneous across input regions, routed experts achieve better alignment with the target function. This motivates training multiple specialized experts, each responsible for a distinct group of subjects.

We employ a Mixture of Experts architecture comprising a router R_0 and multiple routed experts $\{R_j\}_{j=1}^M$. Let $\mathbf{z} = \mathcal{N}_1(\mathbf{x}) \in \mathbb{R}^d$ denote the feature vector extracted from input \mathbf{x} by the feature extractor \mathcal{N}_1 . The output \mathbf{o} is computed as a weighted combination of expert outputs:

$$\mathbf{o} = \sum_{j=1}^M r_j \cdot R_j(\mathbf{z}) \quad (4)$$

where M is the number of routed experts, $R_j(\cdot)$ denotes the j -th routed expert, and r_j represents the routing weight for expert j . The routing weights are sparse, with only the top- K experts receiving non-zero weights.

We adopt a prototype-based routing mechanism. Given feature $\mathbf{z} \in \mathbb{R}^d$, we first project it to a gate dimension space via $W\mathbf{z} \in \mathbb{R}^{d_r}$, then compute the routing weights using cosine similarity with learned prototype embeddings $\mathbf{D} = [\mathbf{d}_1, \dots, \mathbf{d}_M] \in \mathbb{R}^{d_r \times M}$:

$$r_j = \begin{cases} \frac{\exp(\text{sim}(\mathbf{d}_j, W\mathbf{z}))}{\sum_{l \in \mathcal{T}} \exp(\text{sim}(\mathbf{d}_l, W\mathbf{z}))} & \text{if } j \in \mathcal{T} \\ 0 & \text{otherwise} \end{cases} \quad (5)$$

where $\text{sim}(\mathbf{a}, \mathbf{b}) = \mathbf{a}^\top \mathbf{b} / (\|\mathbf{a}\| \|\mathbf{b}\|)$ denotes the cosine similarity, and \mathcal{T} denotes the set of top- K experts with the highest similarity scores. The prototype embedding matrix \mathbf{D} can be interpreted as a codebook for neural activity patterns, and the cosine similarity acts as a matched filter for detecting these patterns. This design mitigates the issue where samples from similar subjects tend to cluster together, enabling each expert to specialize on its assigned cluster.

To optimize the selected experts' predictions toward the ground-truth labels, we employ the cross-entropy loss:

$$\mathcal{L}_{\text{CE}} = -\frac{1}{N_B} \sum_{i=1}^{N_B} \sum_{c=1}^C y_{ic} \log(\hat{y}_{ic}) \quad (6)$$

where N_B is the batch size, C is the number of classes, and $y_{ic} \in \{0, 1\}$ is the ground-truth indicator for sample i belonging to class c .

To encourage each expert to specialize on specific subjects, we compute the average routing probability distribution across all samples from each subject, then minimize the entropy of this distribution:

$$\mathcal{L}_{\text{SL}} = \frac{1}{N_S} \sum_{k=1}^{N_S} H_k, \quad H_k = -\sum_{j=1}^M \bar{r}_{k,j} \log \bar{r}_{k,j} \quad (7)$$

where N_S is the number of unique subjects and $\bar{r}_{k,j} = \frac{1}{|\mathcal{D}_k|} \sum_{\mathbf{x} \in \mathcal{D}_k} r_j(\mathbf{x})$ is the average routing weight for expert j across all samples from subject k , with \mathcal{D}_k denoting the set of samples belonging to subject k . This loss encourages the router to consistently route samples from the same subject to the same expert.

To prevent routing collapse where the model consistently selects only a few experts while leaving others undertrained, we employ an auxiliary balance loss:

$$\mathcal{L}_{\text{BL}} = M \sum_{j=1}^M f_j \cdot \bar{r}_j \quad (8)$$

where $f_j = \frac{1}{N_B} \sum_{i=1}^{N_B} \mathbb{I}[r_j(\mathbf{x}_i) > 0]$ denotes the fraction of samples routed to expert j and $\bar{r}_j = \frac{1}{N_B} \sum_{i=1}^{N_B} r_j(\mathbf{x}_i)$ represents the average routing weight of expert j over the batch. This loss penalizes configurations where a small subset of experts receives disproportionately high routing weights and selection frequencies.

The total loss for routed expert-guided learning is:

$$\mathcal{L}_R = \mathcal{L}_{\text{CE}} + \mathcal{L}_{\text{SL}} + \mathcal{L}_{\text{BL}} \quad (9)$$

3.3 Mutual-Guided Learning

As established in Theorem 3, collaborative learning avoids over-reduction that sacrifices branch-specific information and under-reduction that fails to capture branch-invariant patterns.

For a given sample $\mathbf{x}^{(i)}$ with ground-truth label $y^{(i)}$, let $\ell_S^{(i)} = -\log P_S(y^{(i)}|\mathbf{x}^{(i)})$ and $\ell_R^{(i)} = -\log P_R(y^{(i)}|\mathbf{x}^{(i)})$ denote the cross-entropy losses from the shared expert S_0 and the routed experts $\{R_j\}_{j=1}^M$, respectively. A low loss from the guiding model while the current model produces a high loss

Table 1: Statistics of seven publicly available datasets. We report the task type, total number of subjects, total number of categories, and total number of electrodes. AAD denotes auditory attention decoding, MI denotes motor imagery, and SSD denotes sleep stage detection.

Dataset	Task	Subjects	Categories	Electrodes
KUL (2016)	AAD	16	2	64
DTU (2017)	AAD	18	2	64
AVED (2024)	AAD	20	2	32
BCI IV-2a (2012)	MI	9	4	22
BCI IV-2b (2007)	MI	9	2	3
Sleep-EDFx (2000)	SSD	79	5	2
ISRUC-3 (2016)	SSD	9	5	6

indicates that the sample contains learnable patterns that the current model has not yet captured. A high loss from both models suggests that the sample may be an outlier or contain noise.

When training the routed experts guided by the shared expert, we compute the weighted cross-entropy loss:

$$\mathcal{L}_{R \leftarrow S} = \frac{1}{N_B} \sum_{i=1}^{N_B} (1 + \exp(\ell_R^{(i)} - \ell_S^{(i)})) \cdot \ell_R^{(i)} \quad (10)$$

Samples that the shared expert finds easier (lower $\ell_S^{(i)}$) but the routed experts find challenging (higher $\ell_R^{(i)}$) receive higher weights, constraining the routed experts from under-reduction with guidance from the shared expert.

Similarly, when training the shared expert guided by the routed experts:

$$\mathcal{L}_{S \leftarrow R} = \frac{1}{N_B} \sum_{i=1}^{N_B} (1 + \exp(\ell_S^{(i)} - \ell_R^{(i)})) \cdot \ell_S^{(i)} \quad (11)$$

which assigns higher weights to samples that the routed experts handle well, constraining the shared expert from over-reduction.

The total loss for mutual-guided learning combines both directions:

$$\mathcal{L}_M = \mathcal{L}_{R \leftarrow S} + \mathcal{L}_{S \leftarrow R} \quad (12)$$

4 Experiments

4.1 Experimental Setting

We evaluate the proposed framework on seven publicly available datasets spanning three EEG analysis tasks. For auditory attention decoding, we use the KUL dataset [Das *et al.*, 2016], the DTU dataset [Fuglsang *et al.*, 2017], and the AVED dataset [Fan *et al.*, 2024]. For motor imagery classification, we use the BCI IV-2a dataset [Tangermann *et al.*, 2012] and the BCI IV-2b dataset [Leeb *et al.*, 2007]. For sleep stage detection, we use the Sleep-EDFx dataset [Goldberger *et al.*, 2000] and the ISRUC-3 dataset [Khalighi *et al.*, 2016]. We summarize the statistics of these datasets in Table 1.

For preprocessing, we apply a bandpass filter with cutoff frequencies of 0.1–50 Hz to retain task-relevant neural activity across all datasets, followed by a notch filter at 50 Hz

to remove power line interference. For fair comparison, we follow the experimental protocols of the compared methods for cross-subject cross-validation. For the KUL, DTU, and AVED datasets, EEG signals are segmented into 1-second decision windows with 50% overlap, and we employ leave-one-subject-out cross-validation [Fan *et al.*, 2025]. For BCI IV-2a and BCI IV-2b, EEG signals are segmented into 4-second decision windows without overlap, and we employ leave-one-subject-out cross-validation [Zhao *et al.*, 2024b]. For Sleep-EDFx and ISRUC-3, EEG signals are segmented into 30-second decision windows without overlap [Wang *et al.*, 2024b]; we perform 10-fold cross-validation across subjects for Sleep-EDFx and leave-one-subject-out cross-validation for ISRUC-3. In leave-one-subject-out cross-validation, one subject’s EEG data constitute the test set, while the remaining subjects’ data constitute the training set. In k-fold cross-validation, one fold of subjects constitutes the test set, while the remaining subjects’ data constitute the training set.

We use the Adam optimizer for both the shared expert and the routed experts. The batch size N_B is set to 256, and the maximum number of training epochs is set to 100. Early stopping with a patience of 10 epochs is employed to prevent overfitting. The learning rate is set to 0.0001 for the shared expert and the routed experts. Weight decay is set to 0.0005. Since task-specific models cannot accommodate different tasks with varying topologies and decision windows, we use ListenNet [Fan *et al.*, 2025] for AAD, DeepConvNet [Schirrmeister *et al.*, 2017] for MI, and SleepWaveNet [Wang *et al.*, 2024b] for SSD. The proposed loss function is insensitive to the weighting coefficients; therefore, all coefficients are set to 1. We use $M = 5$ experts and activate one expert at a time. We set $\rho = 10\%$; when the number of electrodes is fewer than 10, we randomly mask temporal segments within the electrodes.

4.2 Comparison Experiments

We first conduct experiments on the auditory attention decoding task using the KUL, DTU, and AVED datasets. We compare the proposed framework with state-of-the-art task-specific models, including CNN [Vandecappelle *et al.*, 2021], SSF-CNN [Cai *et al.*, 2021], MBSSFCC [Jiang *et al.*, 2022], DBPNet [Ni *et al.*, 2024], DARNet [Yan *et al.*, 2024], and ListenNet [Fan *et al.*, 2025]. We also compare with ensemble learning methods, including bagging [Breiman, 1996; Zhang and Zhang, 2008] and boosting, based on ListenNet. As shown in Table 2, the proposed method achieves the best classification accuracy, exceeding 80% on the KUL dataset when combined with ListenNet. Experiments on AAD demonstrate that the proposed method can achieve cross-subject decoding of auditory attention on short segments (1 second) with 10 to 20 subjects.

We then conduct experiments on the motor imagery task using the BCI IV-2a and BCI IV-2b datasets. We compare the proposed framework with state-of-the-art task-specific models, including ShallowConvNet [Schirrmeister *et al.*, 2017], DeepConvNet [Schirrmeister *et al.*, 2017], EEGNet [Lawhern *et al.*, 2018], Conformer [Song *et al.*, 2022], and CT-Net [Zhao *et al.*, 2024b]. We also compare with ensemble learning methods, including bagging [Breiman, 1996;

Table 2: Comparison experiments on the auditory attention decoding task on the KUL, DTU, and AVED datasets under subject-independent conditions. The average accuracy on the test set is reported with leave-one-subject-out cross-validation.

Model	KUL \uparrow	DTU \uparrow	AVED \uparrow
CNN (2021)	56.8	51.8	51.6
SSF-CNN (2021)	59.3	52.3	51.7
MBSSFCC (2022)	62.7	52.5	52.2
DBPNet (2024)	61.1	55.5	52.1
DARNet (2024)	69.9	55.6	51.3
ListenNet (2025)	78.1	56.8	52.8
Bagging (ListenNet)	79.1	57.2	53.2
Boosting (ListenNet)	79.6	57.5	53.1
Proposed (Ours)	81.7	58.3	53.9

Table 3: Comparison experiments on the motor imagery decoding task on the BCI IV-2a and BCI IV-2b datasets under subject-independent conditions. The average accuracy on the test set is reported with leave-one-subject-out cross-validation.

Model	BCI IV-2a \uparrow	BCI IV-2b \uparrow
ShallowConvNet (2017)	56.8	74.3
DeepConvNet (2017)	60.2	75.2
EEGNet (2018)	56.9	75.1
Conformer (2022)	53.4	73.5
CTNet (2024)	58.6	76.3
Bagging (DeepConvNet)	60.6	76.6
Boosting (DeepConvNet)	60.5	76.8
Proposed (Ours)	61.3	77.5

Zhang and Zhang, 2008] and boosting, based on DeepConvNet. As shown in Table 3, the proposed method achieves the best performance with 61.3% four-class accuracy. This demonstrates that the model can perform well even with limited training subjects (9 subjects).

Finally, we conduct experiments on the sleep stage classification task using the Sleep-EDFx and ISRUC-3 datasets. We compare the proposed framework with state-of-the-art task-specific models, including DeepSleepNet [Supratak *et al.*, 2017], Utime [Perslev *et al.*, 2019], TinySleepNet [Supratak and Guo, 2020], SalientSleepNet [Jia *et al.*, 2021], and Sleep-WaveNet [Wang *et al.*, 2024b]. We also compare with ensemble learning methods, including bagging [Breiman, 1996; Zhang and Zhang, 2008] and boosting, based on Sleep-WaveNet. As shown in Table 4, the proposed method achieves the best performance, but the performance gain is smaller compared with AAD and MI. This may be because the cross-subject problem is less severe in SSD; different subjects share patterns such as sleep spindles and K-complexes that are relatively easy to identify with small models, especially given sequential context.

Besides models designed for specific tasks and datasets, we also conduct experiments with deep learning models on multi-task multi-dataset scenarios under subject-independent conditions. Following related work [Zhou *et al.*, 2025b],

Table 4: Comparison experiments on the sleep stage classification task on the Sleep-EDFx and ISRUC-3 datasets under subject-independent conditions. The average accuracy on the test set is reported with subject-wise 10-fold and leave-one-subject-out cross-validation.

Model	Sleep-EDFx \uparrow	ISRUC-3 \uparrow
DeepSleepNet (2017)	81.8	76.5
Utime (2019)	80.6	73.5
TinySleepNet (2020)	82.7	75.8
SalientSleepNet (2021)	82.9	76.9
SleepWaveNet (2024)	83.2	79.2
Bagging (SleepWaveNet)	83.3	79.4
Boosting (SleepWaveNet)	83.5	79.4
Proposed (Ours)	84.1	79.8

we report balanced accuracy. Foundation models include LaBraM [Jiang *et al.*, 2024], CBraMod [Wang *et al.*, 2025], and EEGPT [Wang *et al.*, 2024a]. We apply the proposed method with CBraMod as the backbone. We find that foundation models achieve state-of-the-art performance, while our method can further improve the best foundation model.

4.3 Case Studies

In this section, we conduct case studies to demonstrate in which cases the proposed framework succeeds and in which cases it fails. We train the proposed framework following the same experimental settings as Sec. 4.2 on the KUL dataset. We then report the accuracy of each subject as the test set for the proposed framework, as well as ablated versions with only the shared expert (w/o R) and only the routed experts (w/o S), as shown in Fig. 3.

As shown in Fig. 3, the proposed framework achieves higher performance than the ablated versions for all subjects except subject 16, and also achieves the best overall performance. This indicates that each component contributes to the final performance. For other cases, the shared expert and the routed experts each have their own strengths against over-reduction and under-reduction, and MGEC integrates these strengths.

4.4 Qualitative Analysis

In this section, we conduct qualitative analysis to visualize the learned representations of the shared expert and the routed experts in the feature space. We train the backbone on the BCI-IV-2b dataset with the proposed framework. Then, we use the shared expert and the routed experts to embed the training and test sets, and visualize the embeddings with UMAP.

As shown in Fig. 4, the left subfigure visualizes the embeddings from the shared expert using UMAP for the 1st fold of the training and test sets, and the right subfigure shows the embeddings from the routed experts. We can observe the universal decision boundary of the shared expert. Meanwhile, the six experts reduce to three groups of decision boundaries for the routed experts, where we conduct kernel density estimation to indicate which expert each point is routed to, with the background color corresponding to the assigned expert.

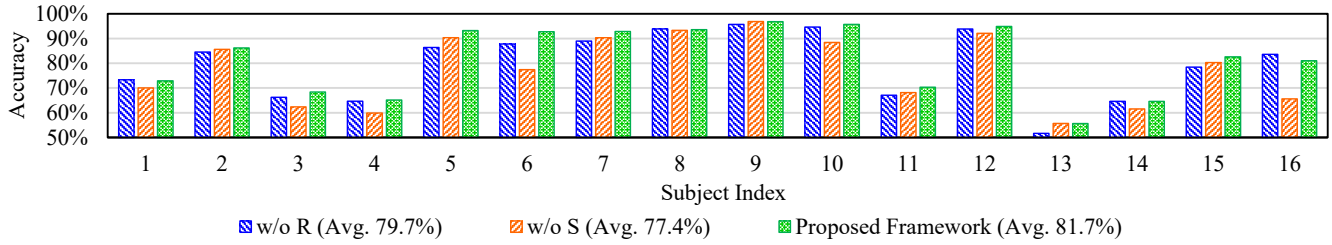
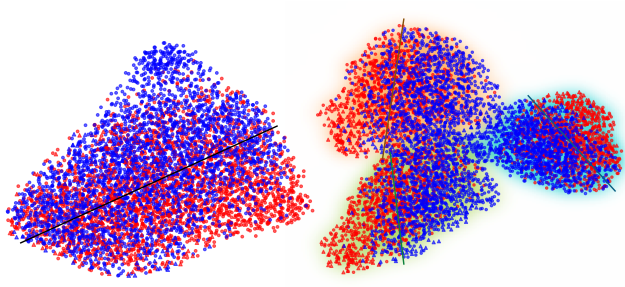


Figure 3: Case studies of the proposed framework on the KUL dataset. The x-axis represents the subject index, and the y-axis represents the accuracy.

Table 5: Comparison of deep learning models on multi-task multi-dataset scenarios under subject-independent conditions. BIOT, LaBraM, and CbraMod are recent EEG foundation models. Balanced accuracy (%) is reported.

Dataset	EEGNet	Conformer	SPaRCNet	ContraWR	CNN-Trans	FFCL	ST-Trans	BIOT	LaBraM	CbraMod	Proposed
KUL	73.7	74.2	73.9	74.1	73.8	73.4	73.6	74.8	75.5	76.5	79.8
DTU	52.3	53.1	52.7	52.9	52.5	52.0	52.4	54.6	55.3	55.6	57.0
AVED	51.7	52.0	51.8	51.9	51.6	51.4	51.5	52.5	52.9	53.8	53.9
BCIC-IV-2a	44.8	47.0	46.4	46.8	46.0	44.7	45.8	47.5	48.7	51.4	56.2
BCIC-IV-2b	75.1	75.6	75.3	75.5	75.2	74.8	75.0	76.0	76.4	76.9	77.6
Sleep-EDFx	77.6	79.2	78.5	78.8	78.1	77.3	77.9	80.8	81.7	82.1	83.2
ISRU	71.5	74.0	74.9	74.0	73.6	72.8	73.8	75.3	76.3	78.7	79.6



• Left Hand (Train) • Right Hand (Train) ▲ Left Hand (Test) ▲ Right Hand (Test)

Figure 4: Qualitative analysis on the BCI-IV-2b dataset. The left subfigure visualizes the embeddings from the shared expert model using UMAP for the 1st fold of the training and test sets, and the right subfigure shows the embeddings from the routed expert model using UMAP for the 1st fold of the training and test sets.

4.5 Synthetic Verification

To empirically validate our theoretical analysis, we construct a synthetic domain generalization dataset. We organize domains into groups, simulating subject groups with similar patterns. Each group has a center sampled from a Gaussian distribution, and each domain within the group has its own center defined as a perturbation from its group center. Samples are then drawn from a Gaussian distribution centered at the domain center.

We define a domain-independent function shared across all domains and a domain-dependent function derived by hierarchically perturbing group-level parameters. The target function for each domain is a weighted combination of the domain-independent and domain-dependent components, where the weight controls the proportion of reducible components.

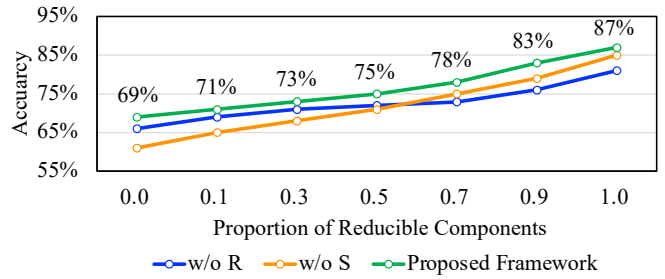


Figure 5: Experiments on synthetic verification under varying proportions of reducible components. We report the target domain test accuracy (%) with different ablation settings.

We use five source domains, where each domain contains 500 samples with an input dimension of 128. We conduct leave-one-domain-out cross-validation. We vary λ from 0 to 1, reporting the target domain test accuracy in Fig. 5. As the proportion of reducible components increases, the routed experts become under-utilized, and shared experts perform better.

5 Conclusion

In this paper, we propose a Mutual-Guided Expert Collaboration framework to address cross-subject generalization in EEG decoding. From a theoretical perspective, we reveal that the optimal coordination of experts depends on the reducibility cost of domain-specific functions to domain-invariant ones. MGECC employs shared experts to capture domain-invariant functions and routed experts to model domain-specific functions, with mutual-guided learning to prevent over-reduction and under-reduction. We validate our findings on synthetic datasets and seven benchmarks.

References

[Berry *et al.*, 2017] Richard B Berry, Rita Brooks, Charlene Gamaldo, Susan M Harding, Robin M Lloyd, Stuart F Quan, Matthew T Troester, and Bradley V Vaughn. Aasm scoring manual updates for 2017, 2017.

[Bomatter and Gouk, 2025] Philipp Bomatter and Henry Gouk. Is limited participant diversity impeding EEG-based machine learning? *NeurIPS*, 2025.

[Breiman, 1996] Leo Breiman. Bagging predictors. *Machine Learning*, 24(2):123–140, 1996.

[Cai *et al.*, 2021] Siqi Cai, Pengcheng Sun, Tanja Schultz, and Haizhou Li. Low-latency auditory spatial attention detection based on spectro-spatial features from eeg. In *EMBC*, pages 5812–5815, 2021.

[Chen *et al.*, 2025] Xinyi Chen, Chenxiang Ma, Yujie Wu, Kay Chen Tan, and Jibin Wu. Neuromorphic sequential arena: A benchmark for neuromorphic temporal processing. *IJCAI*, 2025.

[Das *et al.*, 2016] Neetha Das, Wouter Biesmans, Alexander Bertrand, and Tom Francart. The effect of head-related filtering and ear-specific decoding bias on auditory attention detection. *Journal of Neural Engineering*, 13(5):056014, 2016.

[Fan *et al.*, 2024] Cunhang Fan, Jingjing Zhang, Hongyu Zhang, Wang Xiang, Jianhua Tao, Xinhui Li, Jiangyan Yi, Dianbo Sui, and Zhao Lv. MSFNet: Multi-scale fusion network for brain-controlled speaker extraction. In *MM*, pages 1652–1661, 2024.

[Fan *et al.*, 2025] Cunhang Fan, Xiaoke Yang, Hongyu Zhang, Ying Chen, Lu Li, Jian Zhou, and Zhao Lv. ListenNet: A lightweight spatio-temporal enhancement nested network for auditory attention detection. *IJCAI*, 2025.

[Fuglsang *et al.*, 2017] Søren Asp Fuglsang, Torsten Dau, and Jens Hjortkjær. Noise-robust cortical tracking of attended speech in real-world acoustic scenes. *NeuroImage*, 156:435–444, 2017.

[Goldberger *et al.*, 2000] Ary L Goldberger, Luis AN Amaral, Leon Glass, Jeffrey M Hausdorff, Plamen Ch Ivanov, Roger G Mark, Joseph E Mietus, George B Moody, Chung-Kang Peng, and H Eugene Stanley. Physiobank, physiotoolkit, and physionet: components of a new research resource for complex physiologic signals. *Circulation*, 101(23):e215–e220, 2000.

[Handiru and Prasad, 2016] Vikram Shenoy Handiru and Vinod A Prasad. Optimized bi-objective EEG channel selection and cross-subject generalization with brain-computer interfaces. *Transactions on Human-Machine Systems*, 46(6):777–786, 2016.

[Jia *et al.*, 2021] Ziyu Jia, Youfang Lin, Jing Wang, Xuehui Wang, Peiyi Xie, and Yingbin Zhang. SalientSleepNet: Multimodal salient wave detection network for sleep staging. *IJCAI*, 2021.

[Jiang *et al.*, 2022] Yifan Jiang, Ning Chen, and Jing Jin. Detecting the locus of auditory attention based on the spectro-spatial-temporal analysis of EEG. *Journal of Neural Engineering*, 19(5):056035, 2022.

[Jiang *et al.*, 2024] Weibang Jiang, Liming Zhao, and Bao-liang Lu. Large brain model for learning generic representations with tremendous EEG data in BCI. In *ICLR*, 2024.

[Kessler *et al.*, 2025] Roman Kessler, Alexander Enge, and Michael A Skeide. How EEG preprocessing shapes decoding performance. *Nature Communications Biology*, 8(1):1039, 2025.

[Khalighi *et al.*, 2016] Sirvan Khalighi, Teresa Sousa, José Moutinho Santos, and Urbano Nunes. ISRUC-Sleep: A comprehensive public dataset for sleep researchers. *Computer methods and programs in biomedicine*, 124:180–192, 2016.

[Lawhern *et al.*, 2018] Vernon J Lawhern, Amelia J Solon, Nicholas R Waytowich, Stephen M Gordon, Chou P Hung, and Brent J Lance. EEGNet: a compact convolutional neural network for EEG-based brain–computer interfaces. *Journal of neural engineering*, 15(5):056013, 2018.

[Leeb *et al.*, 2007] Robert Leeb, Felix Lee, Claudia Keinrath, Reinhold Scherer, Horst Bischof, and Gert Pfurtscheller. Brain–computer communication: motivation, aim, and impact of exploring a virtual apartment. *Transactions on Neural Systems and Rehabilitation Engineering*, 15(4):473–482, 2007.

[Li *et al.*, 2018] He Li, Yi-Ming Jin, Wei-Long Zheng, and Bao-Liang Lu. Cross-subject emotion recognition using deep adaptation networks. In *International Conference on Neural Information Processing*, pages 403–413, 2018.

[Li *et al.*, 2023] Bo Li, Yifei Shen, Jingkang Yang, Yezhen Wang, Jiawei Ren, Tong Che, Jun Zhang, and Ziwei Liu. Sparse mixture-of-experts are domain generalizable learners. In *ICLR*, 2023.

[Ma *et al.*, 2019] Bo-Qun Ma, He Li, Wei-Long Zheng, and Bao-Liang Lu. Reducing the subject variability of EEG signals with adversarial domain generalization. In *ICONIP*, pages 30–42, 2019.

[Mienye and Swart, 2025] Ibomoije Domor Mienye and Theo G Swart. Ensemble large language models: A survey. *Information*, 16(8):688, 2025.

[Ni *et al.*, 2024] Qinke Ni, Hongyu Zhang, Cunhang Fan, Shengbing Pei, Chang Zhou, and Zhao Lv. DBPNet: Dual-branch parallel network with temporal-frequency fusion for auditory attention detection. In *IJCAI*, 2024.

[Perslev *et al.*, 2019] Mathias Perslev, Michael Jensen, Sune Darkner, Poul Jørgen Jenum, and Christian Igel. U-time: A fully convolutional network for time series segmentation applied to sleep staging. *NeurIPS*, 32, 2019.

[Rane *et al.*, 2024] Nitin Rane, Saurabh P Choudhary, and Jayesh Rane. Ensemble deep learning and machine learning: applications, opportunities, challenges, and future directions. *Studies in Medical and Health Sciences*, 1(2):18–41, 2024.

[Schalk *et al.*, 2004] Gerwin Schalk, Dennis J McFarland, Thilo Hinterberger, Niels Birbaumer, and Jonathan R Wolpaw. BCI2000: a general-purpose brain-computer interface (BCI) system. *Transactions on Biomedical Engineering*, 51(6):1034–1043, 2004.

[Schirrmeister *et al.*, 2017] Robin Tibor Schirrmeister, Jost Tobias Springenberg, Lukas Dominique Josef Fiederer, Martin Glasstetter, Katharina Eggensperger, Michael Tangermann, Frank Hutter, Wolfram Burgard, and Tonio Ball. Deep learning with convolutional neural networks for EEG decoding and visualization. *Human Brain Mapping*, 38(11):5391–5420, 2017.

[Shen *et al.*, 2022] Xinke Shen, Xianggen Liu, Xin Hu, Dan Zhang, and Sen Song. Contrastive learning of subject-invariant EEG representations for cross-subject emotion recognition. *Transactions on Affective Computing*, 14(3):2496–2511, 2022.

[Song *et al.*, 2022] Yonghao Song, Qingqing Zheng, Bingchuan Liu, and Xiaorong Gao. EEG conformer: Convolutional transformer for EEG decoding and visualization. *Transactions on Neural Systems and Rehabilitation Engineering*, 31:710–719, 2022.

[Sun *et al.*, 2025] Jiangfeng Sun, Kaiwen Xue, Qika Lin, Yufei Qiao, Yifan Zhu, Zhonghong Ou, and Meina Song. Towards recognizing spatial-temporal collaboration of EEG phase brain networks for emotion understanding. In *IJCAI*, pages 3299–3307, 2025.

[Supratak and Guo, 2020] Akara Supratak and Yike Guo. TinySleepNet: An efficient deep learning model for sleep stage scoring based on raw single-channel EEG. In *EMBC*, pages 641–644, 2020.

[Supratak *et al.*, 2017] Akara Supratak, Hao Dong, Chao Wu, and Yike Guo. DeepSleepNet: A model for automatic sleep stage scoring based on raw single-channel EEG. *Transactions on Neural Systems and Rehabilitation Engineering*, 25(11):1998–2008, 2017.

[Tangermann *et al.*, 2012] Michael Tangermann, Klaus-Robert Müller, Ad Aertsen, Niels Birbaumer, Christoph Braun, Clemens Brunner, Robert Leeb, Carsten Mehring, Kai J Miller, Gernot R Müller-Putz, et al. Review of the BCI competition IV. *Frontiers in Neuroscience*, 6:55, 2012.

[Vandecappelle *et al.*, 2021] Servaas Vandecappelle, Lucas Deckers, Neetha Das, Amir Hossein Ansari, Alexander Bertrand, and Tom Francart. EEG-based detection of the locus of auditory attention with convolutional neural networks. *Elife*, 10:e56481, 2021.

[Wang *et al.*, 2024a] Guangyu Wang, Wenchao Liu, Yuhong He, Cong Xu, Lin Ma, and Haifeng Li. EEGPT: Pre-trained transformer for universal and reliable representation of EEG signals. *NeurIPS*, 37:39249–39280, 2024.

[Wang *et al.*, 2024b] Jing Wang, Xuehui Wang, Xiaojun Ning, Youfang Lin, Huy Phan, and Ziyu Jia. Subject-adaptation salient wave detection network for multimodal sleep stage classification. *Journal of Biomedical and Health Informatics*, 2024.

[Wang *et al.*, 2024c] Jiquan Wang, Sha Zhao, Haiteng Jiang, Shijian Li, Tao Li, and Gang Pan. Generalizable sleep staging via multi-level domain alignment. In *AAAI*, volume 38, pages 265–273, 2024.

[Wang *et al.*, 2024d] Xiaotian Wang, Min Dang, Kunkuo Yang, Xinyu Cui, Doudou Zhang, and Chao Chen. The ensemble multi-scale convolution neural network for visual target detection EEG-based brain-computer interfaces. *Biomedical Signal Processing and Control*, 96:106583, 2024.

[Wang *et al.*, 2024e] Yiming Wang, Bin Zhang, and Yujiao Tang. DMMR: Cross-subject domain generalization for EEG-based emotion recognition via denoising mixed mutual reconstruction. In *AAAI*, volume 38, pages 628–636, 2024.

[Wang *et al.*, 2025] Jiquan Wang, Sha Zhao, Zhiling Luo, Yangxuan Zhou, Haiteng Jiang, Shijian Li, Tao Li, and Gang Pan. CBraMod: A criss-cross brain foundation model for EEG decoding. In *ICLR*, 2025.

[Xu *et al.*, 2020] Keyulu Xu, Jingling Li, Mozhi Zhang, Simon S Du, Ken-ichi Kawarabayashi, and Stefanie Jegelka. What can neural networks reason about? In *ICLR*, 2020.

[Yan *et al.*, 2024] Sheng Yan, Cunhang Fan, Hongyu Zhang, Xiaoke Yang, Jianhua Tao, and Zhao Lv. DARNNet: Dual attention refinement network with spatiotemporal construction for auditory attention detection. *NeurIPS*, 37:31688–31707, 2024.

[Zhang and Zhang, 2008] Chun-Xia Zhang and Jiang-She Zhang. Rotboost: A technique for combining rotation forest and adaboost. *Pattern Recognition Letters*, 29(10):1524–1536, 2008.

[Zhang *et al.*, 2024] Hanzhong Zhang, Tienyu Zuo, Zhiyang Chen, Xin Wang, and Poly ZH Sun. Evolutionary ensemble learning for eeg-based cross-subject emotion recognition. *Journal of Biomedical and Health Informatics*, 28(7):3872–3881, 2024.

[Zhao *et al.*, 2024a] Peng Zhao, Ruicong Wang, Zijie Lin, Zexu Pan, Haizhou Li, and Xueyi Zhang. Ensemble deep learning models for EEG-based auditory attention decoding. In *ISCSLP*, pages 339–343, 2024.

[Zhao *et al.*, 2024b] Wei Zhao, Xiaolu Jiang, Baocan Zhang, Shixiao Xiao, and Sujun Weng. CTNet: a convolutional transformer network for EEG-based motor imagery classification. *Scientific reports*, 14(1):20237, 2024.

[Zhou *et al.*, 2025a] Yangxuan Zhou, Sha Zhao, Jiquan Wang, Haiteng Jiang, Shijian Li, Benyan Luo, Tao Li, and Gang Pan. Personalized sleep staging leveraging source-free unsupervised domain adaptation. In *AAAI*, volume 39, pages 14529–14537, 2025.

[Zhou *et al.*, 2025b] Yuchen Zhou, Jiamin Wu, Zichen Ren, Zhouheng Yao, Weiheng Lu, Kunyu Peng, Qihao Zheng, Chunfeng Song, Wanli Ouyang, and Chao Gou. CSBrain: A cross-scale spatiotemporal brain foundation model for EEG decoding. *NeurIPS*, 2025.